



Dynamic coherent perfect absorption in nonlinear metasurfaces

RASOUL ALAEE,^{1,*} YASWANT VADDI,¹ AND ROBERT W. BOYD^{1,2}

¹Department of Physics, University of Ottawa, Ottawa, Ontario K1N 6N5, Canada

²The Institute of Optics and Department of Physics and Astronomy, University of Rochester, Rochester, New York 14627, USA

*Corresponding author: rasoul.alaee@gmail.com

Received 10 July 2020; revised 6 October 2020; accepted 9 October 2020; posted 12 October 2020 (Doc. ID 402380); published 24 November 2020

In this Letter, we propose a tunable coherent perfect absorber based on ultrathin nonlinear metasurfaces. A nonlinear metasurface is made of plasmonic nanoantennas coupled to an epsilon-near-zero material with a large optical nonlinearity. The coherent perfect absorption is achieved by controlling the relative phases of the input beams. Here, we show that the optical response of the nonlinear metasurface can be tuned from a complete to a partial absorption by changing the intensity of the pump beam. The proposed nonlinear metasurface can be used to design optically tunable thermal emitters, modulators, and sensors. © 2020 Optical Society of America

<https://doi.org/10.1364/OL.402380>

An electromagnetic wave carries energy. In many applications in optics (e.g., solar cells, thermal emitters, optical modulators, optical sensors, and optical data processors), it is desirable to absorb light completely [1–5]. In principle, complete light absorption occurs when both reflection and transmission vanish at the same frequency. Perfect absorbers have been proposed after the invention of radar by Salisbury, also known as Salisbury screens [1]. A Salisbury perfect absorber consists of an absorbing layer on top of a metal ground plane separated by a dielectric spacer. Such absorber relies on the destructive interference of the reflected light between the absorbing layer and the metal ground plane (by varying the thickness of the dielectric spacer) and suppression of the transmitted light (due to optically thick metal ground plane).

It is well known that an optically thin metasurface with only an electric dipole response maximally absorbs 50% of the impinging light [2,4–6]. Recently, metasurface perfect absorbers have been introduced using subwavelength resonant particles with *electric and magnetic* responses [4,5,7,8]. These absorbers are thin compared to the operating wavelength and can fully absorb the light without a ground plane. An alternative approach to perfectly absorbing light in an optically thin metasurface with only an electric dipole response is coherent perfect absorber (CPA) by using the interference of two/multiple incoming beams [9–11]. In the CPA, it is essential to choose the intensities appropriately and the relative phases of the two input beams to achieve the perfect absorption. The position of

the metasurface in the standing wave, produced by the interference of two coherent input beams, determines the amount of absorption.

Tunable perfect absorbers have been experimentally and theoretically realized by using tunable materials such as graphene [12–15], liquid crystals [16], and phase-change materials [17–20]. Recently, a new class of low-index materials, called epsilon-near-zero (ENZ) materials, has attracted much attention because of its large nonlinear response [21–26]. As the name indicates, ENZ materials are the materials in which the real part of the permittivity goes to zero at a particular frequency [see Fig. 2(a) for the indium tin oxide (ITO) film]. ENZ materials exhibit a huge electric field enhancement, as well as large nonlinearity at the ENZ frequency [27]. In particular, ITO and aluminum-doped zinc oxide (AZO) as ENZ materials are used to achieve *tunable* antennas and optical switches [21,22,24,26,28]. Perfect absorption has been achieved using the ENZ materials in the linear regime [29–33]. A nearly coherent perfect absorber has been achieved by using Kerr optical nonlinearities in the AZO thin films [34].

In this Letter, we propose an *ultrathin nonlinear* coherent perfect absorber based on an ITO metasurface. In the absence of a pump beam, we show that the metasurface exhibits coherent perfect absorption when illuminated from both sides. The CPA condition, i.e., $t^2 = r_B r_F$, occurs when one of the eigenvalues of the scattering matrix is zero [9]. We demonstrate that the absorber is tunable when applying a third beam (pump beam) with high intensity (see Fig. 1).

The underlying physics of a coherent perfect absorber can be understood using the scattering-matrix formalism [35,36]. The relation between the input \mathbf{a} and output \mathbf{b} waves can be described by $\mathbf{b} = \mathbf{S}\mathbf{a}$, where

$$\mathbf{a} = \begin{pmatrix} a_F \\ a_B \end{pmatrix}, \quad \mathbf{b} = \begin{pmatrix} b_F \\ b_B \end{pmatrix}, \quad \mathbf{S} = \begin{pmatrix} r_F & t_B \\ t_F & r_B \end{pmatrix}. \quad (1)$$

r_F and r_B are the reflection coefficients, t_F and t_B are the transmission coefficients from forward and backward directions, respectively [36]. Coherent perfect absorber occurs when the output waves vanishes, i.e., $\mathbf{b} = \mathbf{0}$ and that is $\mathbf{b} = \mathbf{S}\mathbf{a}_{\text{CPA}} = \mathbf{0}$. This means that at least one eigenvalue of the \mathbf{S} is zero, and the eigenvector is the CPA eigenmode, i.e., \mathbf{a}_{CPA} . For symmetric

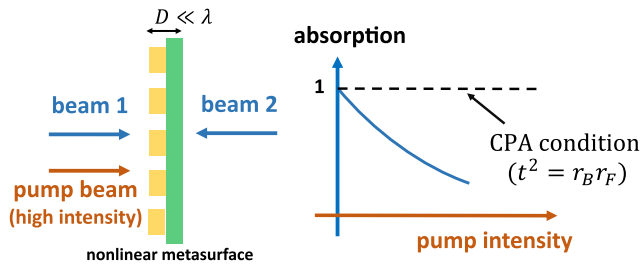


Fig. 1. Main idea of this Letter: a tunable coherent perfect absorber (CPA). Sketch of an ultrathin (i.e., $D \ll \lambda$, where D is the thickness of the metasurface) nonlinear metasurface illuminated by two counterpropagating incident beams. In the absence of a pump beam, the two coherent beams (i.e., beam1, beam2) lead to the CPA when the reflected and transmitted lights destructively interfere on each side of the metasurface. The CPA occurs when Fresnel coefficients satisfy $t^2 = r_B r_F$. Note that single-beam illumination leads to partial absorption [see Figs. 2(e) and 2(f)]. In the presence of the pump, one can modify the absorption by increasing the pump intensity.

structure, the eigenvectors are $(1, \pm 1)$, i.e., the symmetric and antisymmetric input beams. Note that the CPA condition is the time reverse of the lasing [9, 11].

Figure 2(b) shows the schematic of the proposed tunable coherent perfect absorbers. The structure is composed of a gold metasurface 30 nm in thickness on a glass substrate. The ITO layer is sandwiched between the metasurface and the glass substrate. The permittivity of ITO is expressed as $\varepsilon = \varepsilon_\infty - \omega_p^2 / (\omega^2 + i\gamma\omega)$, where $\omega_p = 2.67 \times 10^{15}$ rad/s, $\varepsilon_\infty = 3.9$, and $\gamma = 2.32 \times 10^{14}$ Hz [see Fig. 2(a)]. The transmission spectrum is calculated in Fig. 2(d) for single-beam illumination (forward and backward directions) using a numerical finite element solver (COMSOL Multiphysics). Note that the forward and backward transmissions are identical, i.e., $T = T_F = T_B$ because the system is reciprocal [37]. The structure exhibits strong coupling between two resonances, i.e., the bulk-plasma mode of the ENZ layer and the fundamental mode of the plasmonic nanoantennas [22, 38]. The resonances of the coupled system can be calculated from the eigenvalue problem, i.e., $H\psi = \hbar\tilde{\omega}_{u,l}\psi$, where ψ is the eigenstate of the coupled system, and H is defined as [39]

$$H = \hbar \begin{pmatrix} \tilde{\omega}_{\text{ITO}} & \Delta \\ \Delta & \tilde{\omega}_{\text{MS}} \end{pmatrix}, \quad (2)$$

where $\tilde{\omega}_{\text{ITO}} = \omega_p - i\gamma$ and $\tilde{\omega}_{\text{MS}} = \omega_{\text{LSP}} - i\gamma_{\text{LSP}}$. ω_{LSP} and γ_{LSP} are resonance frequency and linewidth of the localized surface plasmon (LSP) mode of the plasmonic antennas in the absence of the ITO layer, respectively [extracted from Fig. 2(c)]. Δ is the coupling between the bulk-plasma mode of the ITO and the fundamental mode of the metasurface. The coupling Δ is extracted from the simulation of the coupled system. The eigenvalues of the coupled systems are given by

$$\tilde{\omega}_{u,l} = \frac{1}{2} \left(\tilde{\omega}_{\text{MS}} + \tilde{\omega}_{\text{ITO}} \pm \sqrt{(\tilde{\omega}_{\text{MS}} - \tilde{\omega}_{\text{ITO}})^2 + 4\Delta^2} \right). \quad (3)$$

The red and white dashed lines in Fig. 2(d) show the resonance of the metasurface without the ITO and the ENZ wavelength of ITO, respectively. Using Eq. (3), we calculate the resonance wavelengths of the coupled system [see black dashed lines in Fig. 2(d)]. There is a very good agreement between the

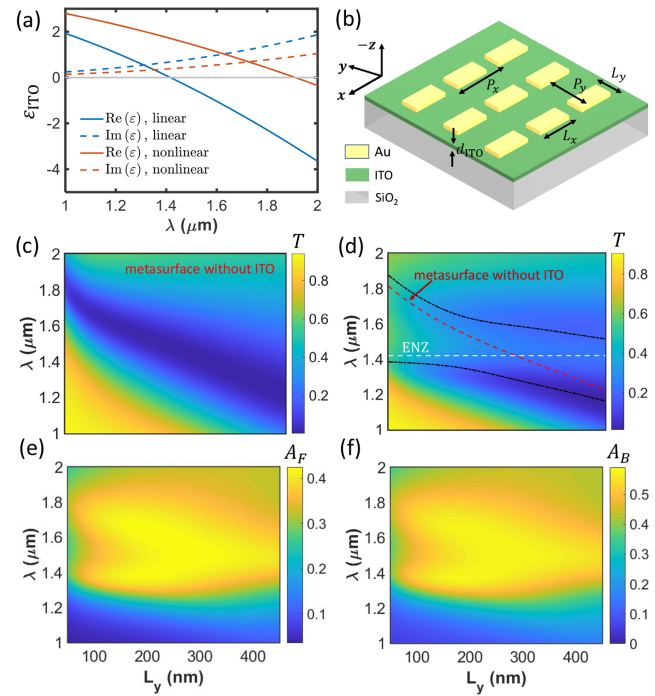


Fig. 2. Single-beam excitation: (a) real and imaginary parts of the linear ($\omega_p = 2.67 \times 10^{15}$ rad/s) and nonlinear ($\omega_{p1} = 2 \times 10^{15}$ rad/s) relative permittivities of the ITO film. (b) Sketch of the tunable perfect absorber consisting of a gold metasurface on top of the ITO-coated SiO₂. The incident plane wave is polarized along the x -axis. (c) Transmission of the metasurface without ITO film as a function of wavelength and dimension of the gold antennas, i.e., L_y . (d) Same as (c) with the ITO film. Note that the dashed lines depict the resonance wavelength of the ENZ, i.e., λ_{ENZ} (white) and the resonance wavelength of the metasurface without ITO, i.e., λ_{MS} (red). Using Eq. (3), the resonance wavelengths of the coupled system, i.e., $\lambda_{u,l}$ can be calculated (see the black dashed lines). (e) and (f) Absorption ($A_{F/B} = 1 - T - R_{F/B}$) for forward ($\mathbf{k}_F = k_0 \mathbf{e}_z$) and backward ($\mathbf{k}_B = -k_0 n_{\text{SiO}_2} \mathbf{e}_z$) illuminations, respectively. The geometrical parameters of the metasurface are $d_{\text{ITO}} = 23$ nm, $P_x = P_y = 650$ nm, and $L_x = 450$ nm. The thickness of the gold nanoantenna is 30 nm.

simulation (using COMSOL) and the semi-analytical model [using Eq. (3)].

Figures 2(e) and 2(f) show the absorption from the forward and backward directions, i.e., $A_{F/B} = 1 - T - R_{F/B}$. $R_F = |r_F|^2$ and $R_B = |r_B|^2$ are reflection from forward and backward, respectively. First, it can be seen that the absorptions (or reflections) are *not* symmetric for the two opposing irradiation directions. The asymmetric reflections/absorptions can be understood from the fact that the system is *not* invariant under space inversion [40–42]. Note that an optically thin metasurface consisting of an electric dipole antennas in an isotropic and homogeneous medium can only absorb 50% of the light [2, 4, 5]. Our proposed asymmetric metasurface is ultrathin, i.e., $\lambda_{\text{res}}/t_{\text{MS}} \approx 30$, where λ_{res} is the resonance wavelength, and t_{MS} is the overall thickness of the metasurface (gold antennas and ITO). Following the approach in [2, 5, 6], we found that the maximum absorption for forward illumination is $A_F^{\text{max}} = n_{\text{air}} / (n_{\text{air}} + n_{\text{SiO}_2}) \approx 0.4$ [see Fig. 2(e)]. Similarly, the maximum backward absorption reads as $A_B^{\text{max}} = n_{\text{SiO}_2} / (n_{\text{air}} + n_{\text{SiO}_2}) \approx 0.6$ [see Fig. 2(f)]. Interestingly, we get $A_B^{\text{max}} + A_F^{\text{max}} = 1$.

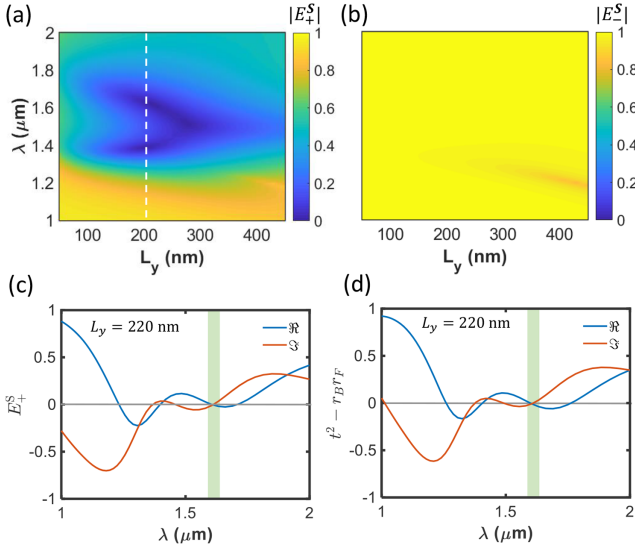


Fig. 3. Coherent perfect absorber condition: (a),(b) Modulus of eigenvalues of the scattering matrix S as a function of wavelength and dimension of the gold antennas. (c) Real and imaginary parts of the eigenvalue of the S -matrix as a function of wavelength for $L_y = 220$ nm. (d) $t^2 - r_B r_F$ as a function of wavelength. The CPA condition occurs at $1.6 \mu\text{m}$. Note that this condition is approximately satisfied over a wide range of wavelengths due to the broadband response of the coupled system.

To find the condition for the coherent perfect absorption, we calculate the two eigenvalues of the scattering matrix, i.e., $E_{\pm}^S = \left(-C_{FB} \pm \sqrt{C_{FB}^2 - 4(r_F r_B - t^2)} \right) / 2$, where $C_{FB} = -(r_F + r_B)$. Thus, the CPA condition, i.e., $t^2 = r_F r_B$ occurs when one of the eigenvalues of S matrix is zero, i.e., $E_+^S = 0$. Figures 3(a) and 3(b) show the modulus of the eigenvalues of E_{\pm}^S matrix as a function of frequency and length of the antenna L_y . It can be seen that only one of the eigenvalues, i.e., E_+^S , vanishes, e.g., at $L_y = 220$ nm [see the white dashed line in Fig. 3(a)]. Figure 3(c) shows that the real and the imaginary parts of the eigenvalue E_+^S are zero at $1.6 \mu\text{m}$ (see the green shadow). At this wavelength, Fresnel coefficients also satisfy $t^2 = r_B r_F$ [see the green shadow in Fig. 3(d)]. Note that the CPA condition is approximately satisfied over a wide range of wavelength due to the broadband response of the coupled system [3,22,38,43]. Therefore, we expect to achieve a nearly broadband CPA for the two-beam illuminations. From now on, we will only consider the metasurface with $L_y = 220$ nm because this geometry satisfies the CPA condition, i.e., $t^2 = r_B r_F$.

Let us now consider the CPA configuration [see the two-beam illumination in Fig. 4(a)]. For the two beams, the joint absorption can be defined as [44]

$$A = 1 - \frac{|b_1|^2 + |b_2|^2}{|a_1|^2 + |a_2|^2}. \quad (4)$$

For lossless systems, absorption is zero $A = 0$, and unity $A = 1$ for the CPA. Figure 4(b) shows the joint absorption for the two-beam illumination as a function of the relative phase of the input beams, i.e., ϕ . By varying the relative phase of the two-beams from 0 to π , the absorption of the metasurface goes

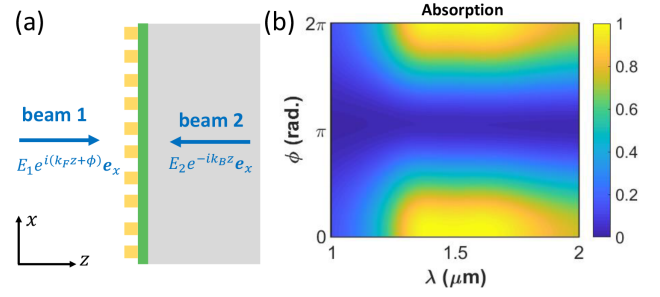


Fig. 4. Two counterpropagating incident beams: (a) schematic representation of the CPA metasurface illuminated by two input beams with low intensities. (b) Absorption as a function of the wavelength and the relative phase between input beams, i.e., ϕ . The CPA occurs when two beams are in phase, i.e., $\phi = 0, 2\pi$. The absorption is nearly zero when two input beams are out of phase, i.e., $\phi = \pi$.

from perfect absorption to nearly zero absorption, while keeping the two beam intensities constant. Note that we used different amplitudes for the incident beams, i.e., $E_2 = 0.86E_1$, which is related to the CPA eigenvector of the a_{CPA} . In other words, the Fresnel coefficients are different because the system is not symmetric. Nearly perfect absorption occurs over a large range of frequencies, i.e., $1.3 - 1.75 \mu\text{m}$ [see also the white dashed line in Fig. 3(a), which depicts the CPA condition]. Figure 4(b) shows that when two beams are out of phase, the absorption is nearly zero because of the vanishing incidence field inside the metasurface.

Next, we consider the effect of a pump beam on the absorption of the proposed nonlinear metasurface. It has been experimentally shown that the refractive index of the ITO depends on the intensity of the pump beam [21,28]. At the high optical intensity regime, ITO's response can be described by the Drude model [21,22,45]. In this model, the plasma frequency of the ITO decreases as the intensity of light increases [21,22,45]. In our simulation, we changed the plasma frequency in the Drude model to model ITO's nonlinearities. Figure 5

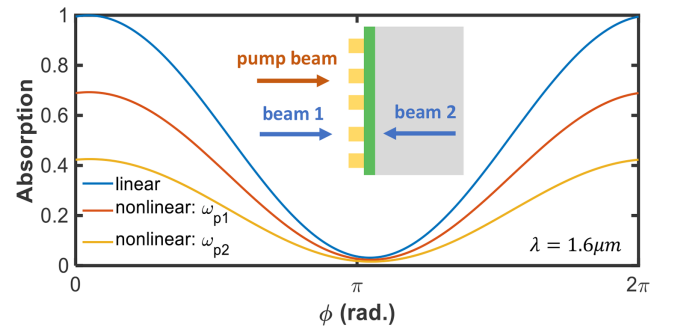


Fig. 5. Two counterpropagating input beams with a pump beam: (a) absorption as a function of the relative phase between two beams at the wavelength $1.6 \mu\text{m}$. The inset shows the sketch of a tunable coherent perfect absorber illuminated by two low-intensity counterpropagating input beams and a high-intensity pump beam. The pump beam changes the refractive index of the ITO. In the nonlinear simulation, we assumed that $\omega_{p1} = 2 \times 10^{15}$ rad/s [see the permittivity of the ITO film in Fig. 2(a)] and $\omega_{p2} = 1.33 \times 10^{15}$ rad/s. Considering the field enhancement in the ITO layer, these plasma frequencies approximately correspond to pump intensities in the range of $I_0 = 1 - 10 \text{ GW/cm}^2$. These are typical intensities that have been reported in the nonlinear experiment with ITO samples [38].

shows the absorption as a function of the relative phase between two beams, i.e., ϕ with and without the pump beam. It can be seen that the absorption is significantly decreased by applying the pump beam (from unity to 0.4) when the relative phase of the two-beams is zero. At $\phi = \pi$, the absorption is almost independent of the pump beam because of vanishing incidence field inside the metasurface. Our proposed CPA is ultrathin ($\lambda_{CPA}/30$, where λ_{CPA} is the CPA wavelength), and its optical response can be switched within a subpicosecond timescale by employing an ultrafast optical pump beam [21].

In conclusion, we have shown that coherent perfect absorption can occur for a metasurface made of optical nanoantennas coupled to an ENZ material. In particular, we have demonstrated that the absorption of the metasurface can be tuned by applying a high-intensity pump beam. Our results can be employed to design tunable thermal emitters, optical modulators, optical sensors, and optical data processes.

Funding. Alexander von Humboldt-Stiftung (Feodor Lynen Fellowship); Canada Excellence Research Chairs, Government of Canada; Canada First Research Excellence Fund; Natural Sciences and Engineering Research Council of Canada; ARO award (W911NF-18-1-0337); Defense Advanced Research Projects Agency (W911NF1810369).

Acknowledgment. R. A. is grateful to M. Karimi, M. Z. Alam, O. Reshef, B. Braverman, A. Safari, and J. Upham for helpful discussions.

Disclosures. The authors declare no conflicts of interest.

REFERENCES

- W. W. Salisbury, "Absorbent body for electromagnetic waves," U.S. patent 2,599,944 (10 June 1952).
- D.-H. Kwon and D. M. Pozar, *IEEE Trans. Antennas Propag.* **57**, 3720 (2009).
- C. M. Watts, X. Liu, and W. J. Padilla, *Adv. Mater.* **24**, OP98 (2012).
- Y. Ra'adi, C. R. Simovski, and S. A. Tretyakov, *Phys. Rev. Appl.* **3**, 037001 (2015).
- R. Alaee, M. Albooyeh, and C. Rockstuhl, *J. Phys. D* **50**, 503002 (2017).
- S. Tretyakov, *Plasmonics* **9**, 935 (2014).
- N. Engheta, in *IEEE Antennas and Propagation Society International Symposium (IEEE Cat. No. 02CH37313)* (2002), Vol. **2**, pp. 392–395.
- N. I. Landy, S. Sajuyigbe, J. J. Mock, D. R. Smith, and W. J. Padilla, *Phys. Rev. Lett.* **100**, 207402 (2008).
- Y. Chong, L. Ge, H. Cao, and A. D. Stone, *Phys. Rev. Lett.* **105**, 053901 (2010).
- W. Wan, Y. Chong, L. Ge, H. Noh, A. D. Stone, and H. Cao, *Science* **331**, 889 (2011).
- D. G. Baranov, A. Krasnok, T. Shegai, A. Alù, and Y. Chong, *Nat. Rev. Mater.* **2**, 17064 (2017).
- R. Alaee, M. Farhat, C. Rockstuhl, and F. Lederer, *Opt. Express* **20**, 28017 (2012).
- S. Thongrattanasiri, F. H. L. Koppens, and F. J. García de Abajo, *Phys. Rev. Lett.* **108**, 047401 (2012).
- Y. Fan, F. Zhang, Q. Zhao, Z. Wei, and H. Li, *Opt. Lett.* **39**, 6269 (2014).
- Y. Fan, Z. Liu, F. Zhang, Q. Zhao, Z. Wei, Q. Fu, J. Li, C. Gu, and H. Li, *Sci. Rep.* **5**, 13956 (2015).
- D. Shrekenhamer, W.-C. Chen, and W. J. Padilla, *Phys. Rev. Lett.* **110**, 177403 (2013).
- M. A. Kats, D. Sharma, J. Lin, P. Genevet, R. Blanchard, Z. Yang, M. M. Qazilbash, D. Basov, S. Ramanathan, and F. Capasso, *Appl. Phys. Lett.* **101**, 221101 (2012).
- T. Cao, C.-W. Wei, R. E. Simpson, L. Zhang, and M. J. Cryan, *Sci. Rep.* **4**, 3955 (2014).
- R. Alaee, M. Albooyeh, S. Tretyakov, and C. Rockstuhl, *Opt. Lett.* **41**, 4099 (2016).
- F. Yang, Y. Fan, R. Yang, J. Xu, Q. Fu, F. Zhang, Z. Wei, and H. Li, *Opt. Express* **27**, 25974 (2019).
- M. Z. Alam, I. De Leon, and R. W. Boyd, *Science* **352**, 795 (2016).
- M. Z. Alam, S. A. Schulz, J. Upham, I. De Leon, and R. W. Boyd, *Nat. Photonics* **12**, 79 (2018).
- L. Caspani, R. Kaipurath, M. Clerici, M. Ferrera, T. Roger, J. Kim, N. Kinsey, M. Pietrzyk, A. Di Falco, V. M. Shalaev, A. Boltasseva, and D. Faccio, *Phys. Rev. Lett.* **116**, 233901 (2016).
- O. Reshef, I. De Leon, M. Z. Alam, and R. W. Boyd, *Nat. Rev. Mater.* **4**, 535 (2019).
- I. Liberal and N. Engheta, *Nat. Photonics* **11**, 149 (2017).
- N. Kinsey, C. DeVault, A. Boltasseva, and V. M. Shalaev, *Nat. Rev. Mater.* **4**, 742 (2019).
- N. Kinsey and J. Khurgin, *Opt. Mater. Express* **9**, 2793 (2019).
- O. Reshef, E. Giese, M. Z. Alam, I. De Leon, J. Upham, and R. W. Boyd, *Opt. Lett.* **42**, 3225 (2017).
- S. Feng and K. Halterman, *Phys. Rev. B* **86**, 165103 (2012).
- K. Halterman and J. M. Elson, *Opt. Express* **22**, 7337 (2014).
- S. Zhong, Y. Ma, and S. He, *Appl. Phys. Lett.* **105**, 023504 (2014).
- T. Y. Kim, M. A. Badsha, J. Yoon, S. Y. Lee, Y. C. Jun, and C. K. Hwangbo, *Sci. Rep.* **6**, 22941 (2016).
- J. Rensberg, Y. Zhou, S. Richter, C. Wan, S. Zhang, P. Schöppe, R. Schmidt-Grund, S. Ramanathan, F. Capasso, M. A. Kats, and C. Ronning, *Phys. Rev. Appl.* **8**, 014009 (2017).
- V. Bruno, S. Vezzoli, C. DeVault, T. Roger, M. Ferrera, A. Boltasseva, V. M. Shalaev, and D. Faccio, *Micromachines* **11**, 110 (2020).
- H. A. Haus, *Waves and Fields in Optoelectronics* (Prentice-Hall, 1984).
- P. Yeh, *Optical Waves in Layered Media* (Wiley, 2005).
- D. Jalas, A. Petrov, M. Eich, W. Freude, S. Fan, Z. Yu, R. Baets, M. Popović, A. Melloni, and J. D. Joannopoulos, *Nat. Photonics* **7**, 579 (2013).
- V. Bruno, C. DeVault, S. Vezzoli, Z. Kudyshev, T. Huq, S. Mignuzzi, A. Jacassi, S. Saha, Y. D. Shah, S. A. Maier, D. R. S. Cumming, A. Boltasseva, M. Ferrera, M. Clerici, D. Faccio, R. Sapienza, and V. M. Shalaev, *Phys. Rev. Lett.* **124**, 043902 (2020).
- V. M. Agranovich, M. Litinskaia, and D. G. Lidzey, *Phys. Rev. B* **67**, 085311 (2003).
- A. Sihvola, A. Viitanen, I. Lindell, and S. Tretyakov, *Electromagnetic Waves in Chiral and Bi-Isotropic Media* (Artech House, 1994).
- R. Alaee, M. Albooyeh, A. Rahimzadegan, M. S. Mirmoosa, Y. S. Kivshar, and C. Rockstuhl, *Phys. Rev. B* **92**, 245130 (2015).
- R. Alaee, J. Christensen, and M. Kadic, *Phys. Rev. Appl.* **9**, 014007 (2018).
- Y. Cui, Y. He, Y. Jin, F. Ding, L. Yang, Y. Ye, S. Zhong, Y. Lin, and S. He, *Laser Photon. Rev.* **8**, 495 (2014).
- L. Baldacci, S. Zanotto, G. Biasiol, L. Sorba, and A. Tredicucci, *Opt. Express* **23**, 9202 (2015).
- H. Wang, K. Du, C. Jiang, Z. Yang, L. Ren, W. Zhang, S. J. Chua, and T. Mei, *Phys. Rev. Appl.* **11**, 064062 (2019).